X-ray cluster surveys and the optical spectroscopic follow-up challenge

Yu-Ying Zhang (Argelander-Institut für Astronomie, Universität Bonn, Germany)

in collaboration with T. H. Reiprich, H. Andernach, C. A. Caretta, P. Schneider, K. Borm, N. Clerc, A. Merloni, A. Schwope & X.-P. Wu

Introduction

— The cluster cosmological applications are degenerate with the mass calibrations of galaxy clusters (e.g. Merloni et al. 2012). Large X-ray surveys select galaxy clusters by their observables (e.g. Ebeling et al. 2000; Böhringer et al. 2004; Clerc et al. 2012; Hilton et al. 2012; Takey et al. 2012), particularly the X-ray luminosity (L), rather than by their masses (M), so that the $L-M$ relation is required to recover the selection function in terms of cluster masses and predict the cluster mass function. Mass estimates from e.g. optical spectroscopy and gravitational lensing, independent of the X-ray luminosity measurement, provide an X-ray blind reference of the cluster mass to calibrate the $L-M$ relation (e.g. Kellogg et al. 1990; Wu et al. 1998; Zhang et al. 2008; Leauthaud et al. 2010; Hoekstra et al. 2014; Mantz et al. 2015).

— Combining X-ray and optical surveys for mass calibration is promising because a vast number of telescopes are dedicated to carry out the optical spectroscopic surveys of galaxy clusters, e.g. eBOSS/SPIDERS (www.sdss3.org/future/eboss.php) and 4MOST (www.4most.eu). The combination of such optical spectroscopic surveys and the X-ray surveys is suitable for cluster cosmology (e.g. Bocquet et al. 2015; Mantz et al. 2015), in which the cosmological parameters and mass calibration are constrained simultaneously based on independent cluster mass observables measured in multi-wavelength surveys.

— Dynamical mass estimates are sensitive to the cluster galaxy selection and member statistic, and overestimate the mass of a merging cluster when one major axis is along the line-of-sight (e.g. Biviano et al. 2006; Old et al. 2013; Saro et al. 2013; Wu & Huterer 2013; Gifford & Miller 2013). Efficient follow-up of cluster galaxies for a large number of galaxy clusters is one of the main tasks in upcoming surveys for high-precision cluster cosmology (e.g. Nandra et al. 2013; Pointecouteau et al. 2013). For optimizing the optical spectroscopy follow-up, it is invaluable to constrain the redshift range those multi-wavelength surveys can provide accurate dynamical masses that are sufficient for the $L-M$ calibration. We simulate the optical spectroscopic follow-up of the HIghest X-ray FLUx Galaxy Cluster (HIFLUGCS, Reiprich & Böhringer 2002) clusters by Monte-Carlo (MC) re-sampling of the cluster galaxy redshifts in hand according to eight optical spectroscopic setups. We calibrate the dynamical mass estimates and quantify in which redshift range the tested optical spectroscopic setups are reliable for measuring the cluster dynamical masses.

HIFLUGCS Sample: calibrating X-ray luminosity as mass proxy with dynamical mass

Sample and analysis: We performed the mass calibration for the HIFLUGCS sample based on high-quality *XMM-Newton* and *ROSAT* pointed observations as well as optical spectroscopic redshifts of more than ten thousand cluster galaxies (Zhang et al. in prep.). We carried out the X-ray and optical analyses independently (Zhang et al. 2011), apart from taking the dynamical mass determined r_{500} in computing the X-ray luminosity. Since the luminosity values measured within r_{500} and $2.5r_{500}$ differ only by $\sim$10% on average, using the r_{500} derived from the dynamical mass, in computing the X-ray bolometric luminosity will not cause any significant bias in our result.

Fig. 1: Core-corrected X-ray bolometric luminosity versus dynamical mass with the best power-law fits for the 63 and 57 ($n_{\rm gal} \geq 45$) clusters as black solid and dashed lines. Filled triangles and open boxes denote cool core (CC) and non-cool core (NCC) clusters. Disturbed and undisturbed clusters are in blue and red. The magenta line is from a simultaneous fit to the $L-M$ relation and cosmological parameters (i.e. Ω_m and σ_8) for the whole sample taking into account the selection function.

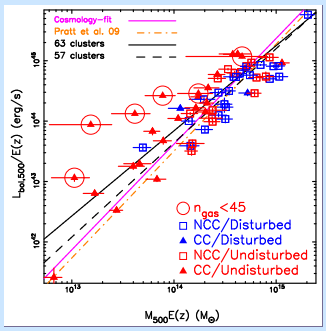

Fig. 1

Summary:

We calibrated the $L-M$ relation using the dynamical mass derived independently from the X-ray luminosity.

Our result for the whole sample from the simultaneous fit to the $L-M$ relation and cosmological parameters (Ω_m and σ_8) taking into account the selection function agrees with the recently X-ray self-calibrated relations (e.g. Pratt et al. 2009).

Given sufficient numbers (i.e. $\geq$45) of member galaxies in computing the dynamical masses, the $L-M$ relations agree between the disturbed and undisturbed clusters. With low numbers of cluster galaxies, the dynamical masses tend to be underestimated.

The CC clusters still dominate the scatter in the $L-M$ relation although the CC corrected X-ray luminosity is used. It indicates that the scatter of the $L-M$ scaling relation mainly reflects the structure formation history.

Down-sampling of the HIFLUGCS sample using the eBOSS/SPIDERS and 4MOST configurations

Optical spec-z survey configurations: Both large optical spectroscopic surveys and individual pointed observations will be used to follow up galaxy clusters detected in upcoming large X-ray surveys, e.g. *eROSITA* and *Athena*. We calibrated the dynamical mass estimates according to different spectroscopic survey setups, and demonstrate here the results for the following two follow-up programs of the *eROSITA* detected clusters. The Extended Baryon Oscillation Spectroscopic Survey (eBOSS; e.g. Schlegel et al. 2011) is a redshift survey covering a wavelength range from 340 nm to 1060 nm, with a resolution R =3000–4800. This survey targets objects up to redshift 2. With the eBOSS setup, the SPectroscopic IDentification of ERosita Sources (SPIDERS; e.g. Merloni et al. 2012) survey will take optical spectra of 50,000 X-ray emitting quasars and galaxies in the northern X-ray clusters detected by *eROSITA*. The 4-metre Multi-Object Spectroscopic Telescope (4MOST, e.g. de Jong et al. 2012) is designed to obtain more than 20 million spectra at resolution $R\sim$5000 ($\lambda = 390-1000$nm) and more than two million spectra at $R\sim$20,000 (395–456.5 nm & 587–673 nm) within five years. It is suitable to follow-up the clusters in the southern sky in the *eROSITA* survey.

Analysis: In practice, only a number of cluster galaxies per cluster can be targeted given a fiber spacing constraint. Toward the high-redshift regime, a bright limiting magnitude cut can strongly limit the number of spectroscopic members. We correct apparent magnitudes for Galactic extinction using the maps of Schlegel et al. (1998). We use typical colors and their color uncertainties of luminous red galaxies of Maraston et al. (2009), and apply K-correction and evolutionary correction using the luminous red galaxy template in kcorrect (v4_2, Blanton & Roweis 2007). To estimate the average of the systematic uncertainties, we carried out 500 re-sampling runs per cluster per survey configurations per input cluster redshift ($z_{\rm in} = z, 0.2, 0.4, 0.6, 0.8$). In each run, we measured the cluster redshift, velocity dispersion and dynamical mass. Otherwise ($n_{gal,i} < 10$), we only compute the cluster redshift, which is the mean of the member galaxy redshifts, but not the velocity dispersion and dynamical mass.

Fig. 2: Dynamical mass from the down-sampling normalized by the input dynamical mass (solid curves) and its 1-σ dispersion (dashed curves) as a function of the re-sampled number of redshifts per cluster in the eBOSS/SPIDERS (upper panel) and 4MOSTmag (lower panel) configurations. The curves in different colors present the cases when the cluster sample was placed at the original cluster redshifts, $z = 0.2$, $z = 0.4$, $z = 0.6$, and $z = 0.8$, respectively. The dispersion was estemated from the 500 re-sampling runs per cluster per survey configurations per input cluster redshift.

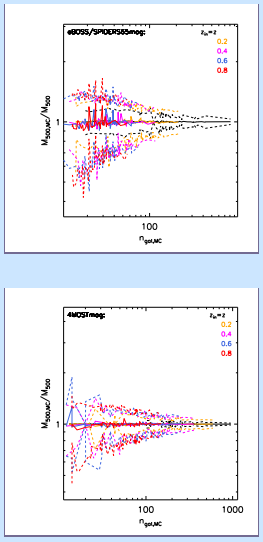

Fig. 2.

Summary:

The dispersion of the dynamical mass from the down-sampling normalized by the input dynamical mass as a function of the re-sampled number of redshifts can be useful for the sample selection and follow-up planning corresponding to the required precision for the purpose of mass calibration in upcoming surveys.

With ten redshifts per cluster, the dynamical masses can be recovered to 20% level on average, in which the dynamical masses are underestimated for most systems, and can easily be biased by a factor of two for individual clusters.

The bias of the cluster dynamical mass estimates increases toward the high-redshift end. The underestimation of the cluster masses on average using the eBOSS/SPIDERS setup is better than 19%, 28%, 34%, and 37% at $z = 0.2$, 0.4, 0.6, and 0.8. The dynamical mass is recovered with less than 20% underestimation up to redshift 0.6 using the 4MOST setup. At the redshift bin of 0.8, the underestimation of the dynamical masses on average according to the 4MOST setup is better than 24%. Assuming the eBOSS/SPIDERS (4MOST) setup, the dynamical masses can be used as an independent reference blind to the X-ray observables to calibrate the cluster mass to better than 20% precision up to redshift 0.2 (0.6) with 2% (3%) catastrophic outliers in upcoming X-ray surveys.

Acknowledgments:

YYZ acknowledges support by the German BMBF through the Verbundforschung under grant No. 50 OR 1304 and 50 OR 1506.

Selective references:

Biviano et al. 2006, A&A, 456, 23
Blanton & Roweis, 2007, AJ, 133, 734
Bocquet et al. 2015, ApJ, 799, 214
Böhringer et al. 2004, A&A, 425, 367
Clerc et al. 2012, MNRAS, 423, 3561
de Jong et al. 2012, arXiv:1206.6885
Ebeling et al. 2000, MNRAS, 318, 333
Gifford & Miller 2013, ApJ, 768, L32
Hilton et al. 2012, MNRAS, 424, 2086
Kellogg et al. 1990, GL, 360, 141
Leauthaud et al. 2010, ApJ, 709, 97
Mantz et al. 2015, MNRAS, 446, 2205
Maraston et al. 2009,MNRAS, 394, L107
Merloni et al. 2012, arxiv1209.3114
Nandra et al. 2013, arXiv1306.2307
Old et al. 2013, MNRAS, 434, 2606
Pointecouteau et al. 2013, arXiv1306.2319
Pratt et al. 2009, A&A, 498, 361
Reiprich & Böhringer 2002, ApJ, 567, 716
Saro et al. 2013, ApJ, 772, 47
Schlegel et al. 1998, ApJ, 500, 525
Schlegel et al. 2011, arXiv1106.1706
Takey et al. 2013, A&A, 558, A75
Wu et al. 1998, A&A, 338, 813
Wu & Huterer, 2013, MNRAS, 434, 2556
Zhang et al. 2008, A&A, 482, 451
Zhang et al. 2011, A&A, 526, A105